UNITED STATES DEPARTMENT OF THE INTERIOR

GEOLOGICAL SURVEY

FAST-ICE THICKNESS AND SNOW DEPTH IN RELATION TO OIL ENTRAPMENT POTENTIAL, PRUDHOE BAY, ALASKA

OPEN-FILE REPORT 79-539

This report is preliminary and has not been edited or reviewed for conformity with Geological Survey standards and nomenclature

Menlo Park, California

1979

UNITED STATES
DEPARTMENT OF THE INTERIOR
GEOLOGICAL SURVEY

FAST-ICE THICKNESS AND SNOW DEPTH IN RELATION TO OIL ENTRAPMENT POTENTIAL, PRUDHOE BAY, ALASKA

By Peter W. Barnes, Erk Reimnitz, Lawrence J. Toimil, and Harry R. Hill

---

Open-File Report 79-539

Menlo Park, California
March 1979

Fast-ice Thickness and Snow Depth in Relation to Oil Entrapment Potential, Prudhoe Bay, Alaska

Peter W. Barnes, Erk Reimnitz, Lawrence J. Toimil, and Harry R. Hill

ABSTRACT

In winter, the undersurface of the sea ice on shallow arctic shelves acts upon the sea bed directly by contact and indirectly by influencing currents and turbulence. The under-ice surface would serve as a trap for pollutants such as oil and gas released from the sea bed. A knowledge of the morphology of the undersurface of the ice is a first step in understanding the sea-bed interactions and in evaluating the quantities, configuration, and dispersal patterns of sub-ice pollutants. Investigations show thicker sea-ice correlates with a thin snow cover and thin sea-ice underlies elongate snow ridges.

In early May, 1978, the relationships between under-ice morphology, sea bed morphology, tidal currents, and variations in snow thickness were studied. At three sites representing three different environments--protected bay, deep, open lagoon, and narrow tidal channel--trenches were cut through the ice. The trenches were parallel and perpendicular to the sastrugi-sculptured northeast-southwest trending snow ridge pattern. Snow depth, ice thickness, and ice drafts were measured and an upward-directed side-scanning sonar was towed to examine the morphology of the under-ice surface in an area 100 m square.

Snow depth and ice thickness vary about 30-40 cm and exhibit a negative correlation--thin ice coinciding with a thicker insulating snow cover. The areal snow and ice morphology patterns reinforced the correlation. Elongate ridge and trough patterns on the under-ice

surface parallel the surface snow ridge patterns on wavelengths typically 10 m wide, yielding sub-ice voids of 25 to 47 x $10^3 m^3/km^2$ (600-1200 barrels per acre). Diving observations indicate a smaller set of depressions 5 cm or less in depth, oriented parallel to the ice crystal fabric, and an escape of sub-ice released air to the snow-ice interface.

The results imply that there is a seasonal stability to the snow ridge pattern and that oil concentrations under the ice would be indicated by surficial snow morphology in the fast ice zone. Spreading directions would be enhanced in the elongate dimensions of the under-ice ridges and troughs, that is, upwind and downwind. In spring, gases will leak to the surface.

INTRODUCTION

The undersurface of sea ice on arctic shelves interacts with the sea bed directly and indirectly by the disruptive processes associated with ice gouging and by influencing currents and turbulence. Furthermore, the under-ice surface serves as a trap for floating pollutants released from the sea bed in winter. A knowledge of the morphology of the undersurface of the ice is a first step in understanding the sea-bed interactions and in evaluating the quantities, configuration, and dispersal patterns of sub-ice pollutants.

In this report we discuss the three-dimensional morphology of sea ice at three sites on the fast ice in the Prudhoe Bay area. At each of the sites - protected bay, open lagoon, and tidal channel - snow depth and ice thickness show a negative correlation, reflecting the insulation of the ice by snow and a seasonal stability to the snow ridge patterns on the sea-ice surface.

Background

Ice Environment

The studies which form the basis of this report were all conducted in the fast-ice zone. This ice zone is a seasonal ice formation which is essentially immobile in winter, forming an extension of the land surface (Kovacs and Mellor, 1974, p. 116). Depending on the snow cover and local temperature regime, fast-ice growth is initiated in September or October, growing at a rate of about 1 cm per day, reaching thicknesses of 2 m by the end of the growth season in March or April (Kovacs and Mellor, ibid; Schell, 1974, p. 231). Seaward extent of fast ice is controlled by water depth, the protection afforded ice by the shoreline, the time available for growth of the fast ice, and the magnitude and intensity of pack ice movement on the inner shelf (Kovacs and Mellor, p. 117). The character of the fast ice is affected by atmospheric and oceanographic conditions at the time of freezing. Currents, waves, and winds at the time of freezing cause the initial fast-ice surface to be rough whereas calm conditions during freeze-up cause a smooth surface (Kovacs and Mellor, ibid). Early winter storms can also dislodge and reorient sections of the fast ice if the ice has not yet achieved sufficient strength to withstand these forces.

Snow Cover

Benson and his coworkers (1975, p. 13) have noted that the snow cover along the arctic coast of Alaska is similar to that of Greenland and Antarctica, being characterized as hard, high density, wind-packed snow, overlying a low density snow. These workers also note that wind drifts are formed in response to the prevailing northeasterlies. In the

fall, at wind speeds of 12 to 20 m per second, snow ridges form as stationary features parallel to prevailing winds--30 to 60 m long, 10 to 20 cm high, and 6 to 8 m wide (Kruchinin, 1962). Snow ridges are subsequently scoured, forming steep-faced erosional features called sastrugi which are common through the remainder of the winter. Eroded snow together with additional precipitation form snow spots, irregularly shaped patches of soft snow approximately 10 m in diameter and 10 cm deep, or snow barchans which move under the influence of the prevailing winds across the more stable snow ridges (Kruchinin, p. 78). In the Canadian arctic, Brown and his associates (1975, p. 70) noted that snow ridge patterns, formed on the fast ice in fall, remained intact throughout the winter. They noted the average depth of the snow on the fast ice by the end of winter was about 22 cm, while at Prudhoe Bay the tundra snow depth has been observed to average 32 cm (Benson and others, 1975).

Oceanography

The oceanography of the fast-ice zone in winter is affected by the formation of an ice cover as well as by the presence of an ice cover. The process of freezing of sea water excludes brines so that the ice is of a much lower salinity than the waters from which it is formed. This has resulted in notable increases in the salinities of sub-ice waters in bays and lagoons where circulation is restricted (Schell, 1974, p. 240; Kovacs and Mellor, 1974, p. 117). Values of salinity in excess of 50°/oo have been reported in these environments (Schell, 1974). The presence of an ice cover dampens waves and removes the influence of wind as a current driving force. Tidal currents generated by the 15-20 cm tides can be intensified in inlets by the decrease in cross sectional area due to ice growth.

Previous Work

The fact that snow depth influences ice thickness has been known for some time (Zubov, 1943, p. 220). However, the magnitude of influence and the variability, have received minimal attention. Canadian studies of fast ice have shown that ice thickness is inversely related to snow depth and that ice thickness varies by about 20% of the mean thickness (Brown and others 1975, p. 36). A 35 cm maximum difference in fast ice thickness at the end of the 1974-75 growth season was noted. Furthermore the snow drift pattern remained stable all winter once established in fall. These observations were then used to to develop heat transfer equations for ice, snow, and oil mixtures (Brown and others, 1975, p. 74).

Kovacs (1977) measured fast ice thicknesses along a linear profile using electromagnetic techniques and found variabilities of 30 cm or about 25% of the mean thickness (Kovacs, 1977, p. 548); but he did not relate this variability to snow cover. Kovacs (1977, p. 549) calculated potential volume of oil trapped in the voids on the undersurface of the ice (above his observed mean thickness) at 27,500 m^3/km^2.

Methods

From 29 April to 15 May, 1978, field studies were undertaken in the Prudhoe Bay area using a variety of techniques. At each of three sites a cross was staked out in the snow with one arm perpendicular to the dominant trend of surficial snow ridges. Each arm was 100 m long and intersected the cross arm at 50 m. After the cross was marked with flags and stakes, snow depths were measured at 5 m intervals. Aerial photographs were taken from altitudes of 200 to 300 m. Subsequently an

access road was plowed to each site and the sea ice was cleared of snow for several meters on either side of the cross. A mechanical ditching machine was then used to cut a 20-cm-wide, 100-m-long trench through the ice along a transect corresponding to the cross initially marked in the snow. A 1.5 m^2 block of ice was cut by the ditcher and lifted out with a fork lift to form a dive hole. The ditcher did not remove the bulk of the chips during trenching so that it was necessary to perform the tedious task of "mucking out" the trench and dive hole. The character of prepared sites is shown in Figure 1.

After the site had been cleared, a sled was propelled by hand over the trench. Sensors suspended from the sled - which also carried the electronics and recorders--included upward-directed side-scanning sonar, precision fathometer, pressure transducers, and underwater television. Ice thickness and freeboard (water level to upper ice surface) were measured at 2-m intervals along the trenches. Sub-ice temperature and salinities were measured with a conductivity bridge which has a temperature accuracy of $0.5^{\circ}C$ and a salinity accuracy of $0.3^{\circ}/oo$.

A time lapse camera was mounted on a structure near the Arco west dock. The camera view was eastward, and exposures were obtained at 15 minute nominal intervals. Only two days of useable record were obtained--partly due to camera failure but primarily due to blowing snow or fog which obscured the camera view.

Site Descriptions

Three differing ice and oceanographic environments in the fast-ice zone were examined; one in the shallow, protected environment of Prudhoe Bay; one in the deeper, open environment of Stefansson Sound; and one in a deep, narrow tidal inlet to Simpson Lagoon between Egg Island and Long Island, as shown in Figure 2.

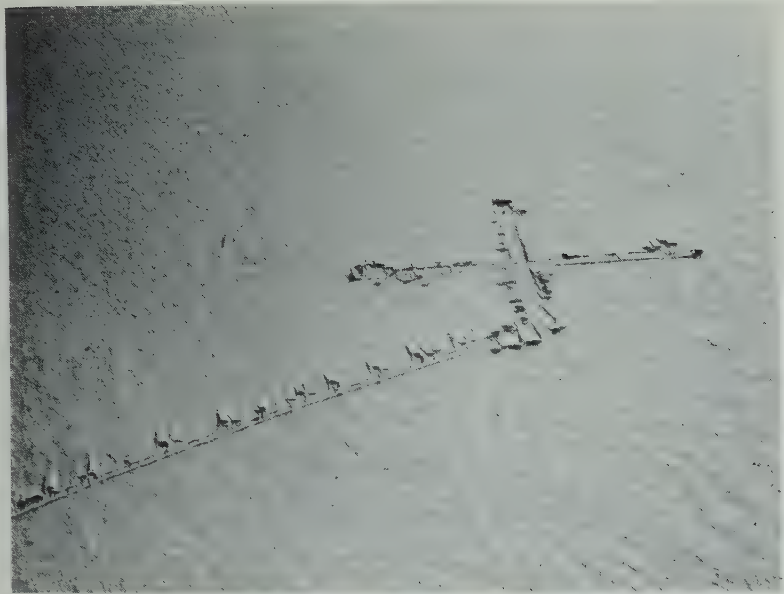

a

b

c

Figure 1. a) Aerial view of site 1 showing the fast ice and the access road after all work was completed. Note the alignment of the cross with the elongate snow ridge pattern and the drifts in the lee of snow piles. b) View along easterly arm of the cross at Site 1 showing the clean trench and sea-ice surface. The large ice block seen at the end of the trench has been removed from the dive hole. Note the variability in ice freeboard along the trench. c) Aerial view of Site 3 showing the orientation and relation of the site to the spit at the southern tip of Long Island (see Fig. 2). Just to the right of the people near the center of the cross is one of the dive holes at this location.

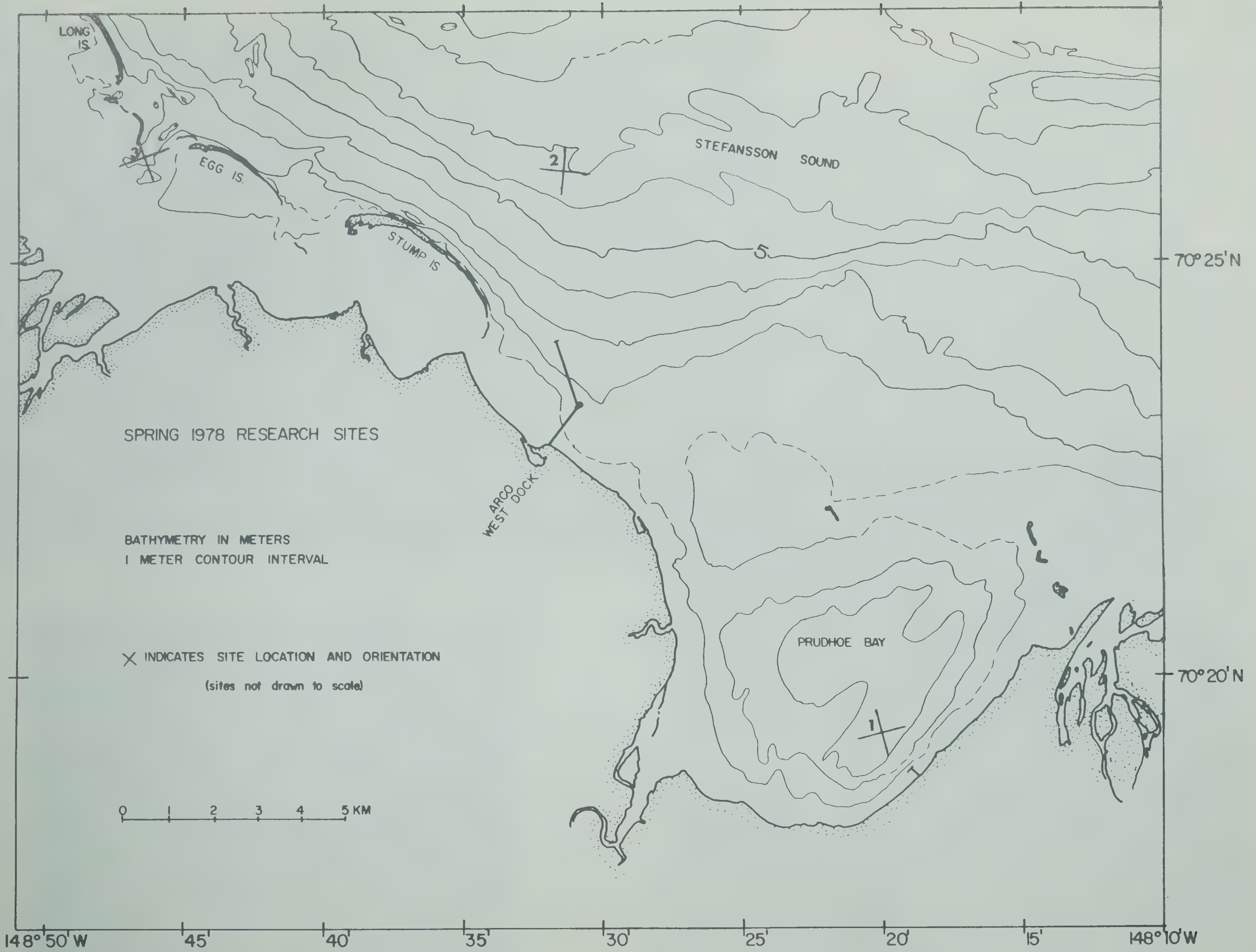

Figure 2. Locations of test sites and their relation to geography and bathymetry.

The Prudhoe Bay site (Site 1) is located in a semi-enclosed coastal embayment. Depths in the central part of the embayment approach 4 m, although the deepest channel connecting the bay with the open ocean is less than 2 m deep (Barnes and others, 1977). Bay waters are free to communicate with the offshore oceanic environment during the summer, and is essentially oceanic in character at the time of freeze-up. Lateral ice motion within the bay is almost non-existent once a solid ice canopy has formed late in fall. With the formation of the ice canopy, circulation is restricted so that by the time of our field studies in spring, sub-ice waters were less than $-2^{\circ}C$ in temperature and greater than $64^{\circ}/oo$ in salinity. At the time of our fieldwork the undersurface of the ice was less than 2 m from the sea bed and thermal, brine drainage, tidal or current intensification influence on the sea bed due to ice was thought to be most pronounced. Vertical ice motions due to tidal interchange through the channel during winter, as proposed by Barnes and others (1977, p. 12), were not observed at a nearby ice level recording station. In summary, the Prudhoe Bay site was characterized by high salinities, a close proximity of the under-ice surface to the sea bed, extremely weak sub-ice currents, and an absence of large lateral or vertical motions of the ice canopy.

The Stefansson Sound site (Site 2), with water depths greater than 5 m, is a deeper, more open environment than the Prudhoe Bay site. Lateral ice motion in Stefansson Sound probably occurred during the early winter as evidenced by the blocky, irregular, and justaposed ice patches along the road plowed to the site. The sub-ice waters are free to communicate with the ocean throughout the winter and temperatures of

$-2^{\circ}C$ and salinities of $38^{\circ}/oo$ were recorded. In spring, 1972, we measured weak sub-ice currents towards the northwest at 2 cm per second or less at a station 7 km west of Site 2. In summary, at this site the ice canopy is well away from the influence of the bottom and sub-ice water is calm with minimal currents. The lateral motion of ice during most of the ice growth season is insignificant, being protected by the island chain to the northeast.

The third site, between Egg Island and Long Island, (Site 3), represents a narrow, 5-m deep, tidal channel between a shallow lagoon and the more open shelf. In spring, 1972, we measured tidal currents of up to 20 cm per second in this channel (Fig. 3). During the present study, vertical ice motion of up to 20 cm with tidal period was recorded adjacent to this site, attesting to the interchange of lagoon and open ocean water areas where sub-ice currents are intensified and are known to reduce ice thickness (Zubov, 1943, p. 222). Observations at Site 3 in spring show the inlet to have open water earlier in the spring than elsewhere as shown in Figure 4. Sub-ice waters were observed to be $-1.6^{\circ}C$ and to have a salinity of $38^{\circ}/oo$, an increase of at least 10% over summer salinities (Barnes and others, 1977, p. A-9), perhaps representing brine drainage from the ice freezing process within the lagoon although these values were also observed at Site 2. Lateral ice motion in the inlet is thought to be minimal although stresses are suggested by ice push onto the beach at the western edge of the site, and the numerous cracks up to 5 cm wide noted at the snow and ice surface. In summary, this site is one where ice growth and sub-ice salinities could be influenced by a lagoonal ice canopy, where ice motion was expected to be minimal, and where the effects of current were expected to be pronounced.

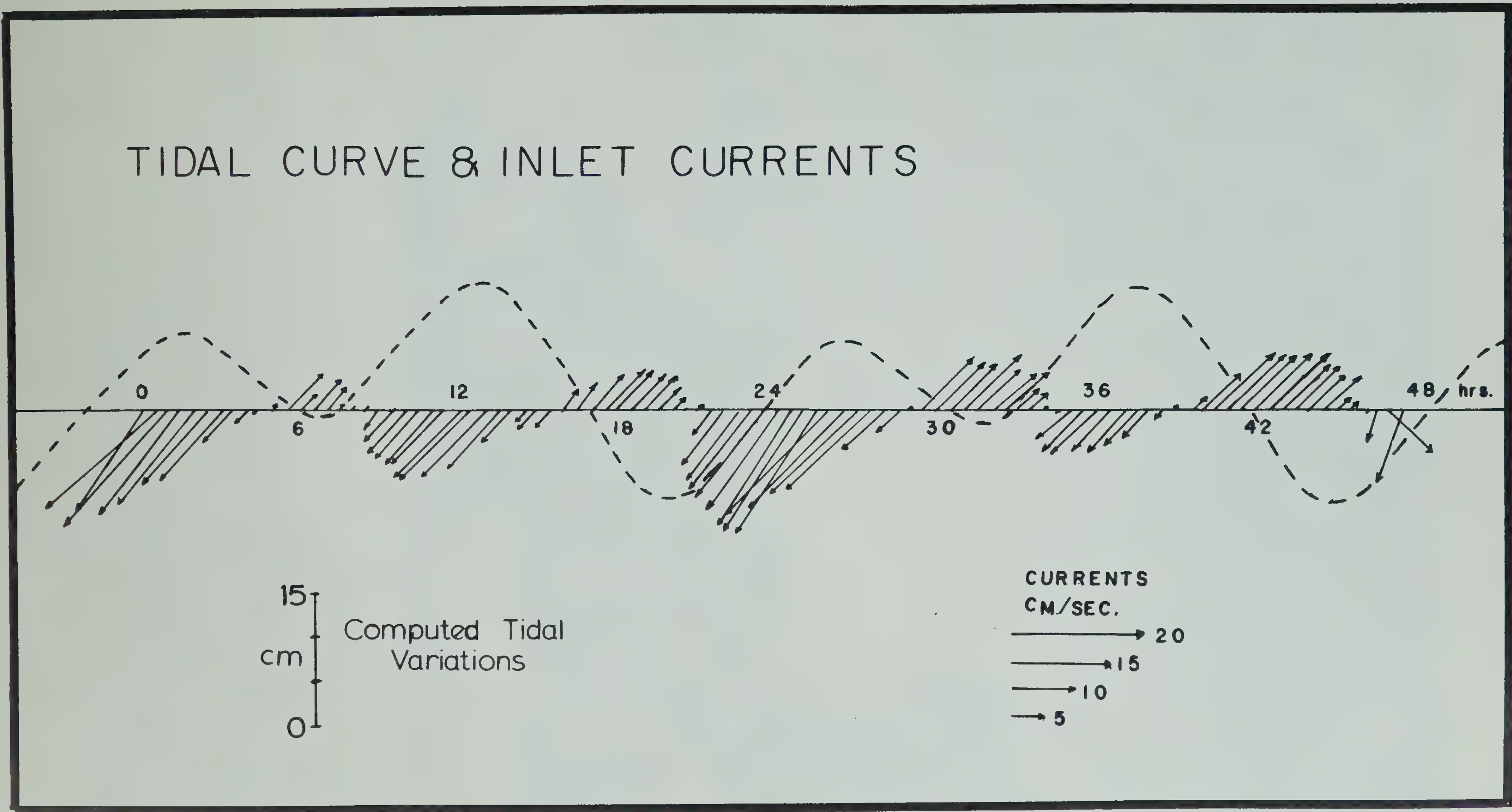

Figure 3. Mean half-hourly currents measured 50 cm below the fast ice during late May, 1972 at the tidal inlet between Egg Island and Long Island (Site 3). Superimposed tidal curve was taken from computed data from Flaxman Island 70 km to the east.

Figure 4. Aerial photograph of the coast and inner shelf just west of Prudhoe Bay taken in June, 1974. Ice is present offshore and in the lakes. Note the open water at the tidal inlet (Site 3) and the uniform character of the ice nearshore in comparison to further offshore in Stefansson Sound.

RESULTS

Correlation of Snow Depth and Ice Thickness

Reconstructions of snow depth, ice thickness, and ice freeboard (distance from the water level to the ice surface) along the trenches illustrate the relationship of snow depth to ice thickness. Thin ice, low freeboard, and deep snow are consistently related, both parallel to, and perpendicular to, the snow ridge pattern (Figure 5 and Table I).

Snow depths averaged 15 to 24 cm but ranged from 4 cm to 48 cm at the three study sites. Site 2 had on the average 10 cm less snow than other sites. The average, maximum, and minimum snow depths were similar on transects both perpendicular and parallel to the snow ridge pattern (Table I).

Ice thickness at the three study sites averaged between 134 cm and 157 cm but ranged from 114 cm to 169 cm. The ice was thinnest at Site 1 but essentially the same at Sites 2 and 3 (Table I). In most cases the upper ice surface shows isostatic adjustment to thickness--less freeboard is associated with thinner ice and deeper snow.

Statistical consideration suggests that less range in both snow depth and ice thickness would be observed along transects parallel to the snow ridges than at right angles as fewer ridges and troughs would be encountered in the sample. Snow depth shows this relationship only at Sites 1 and 3, although ice thickness shows a smaller range parallel to the snow pattern only at Sites 1 and 2; but in both cases the differences are 30% or less.

As a test for snow depth-ice thickness correlation, graphs were plotted for total snow depth versus total ice thickness using data

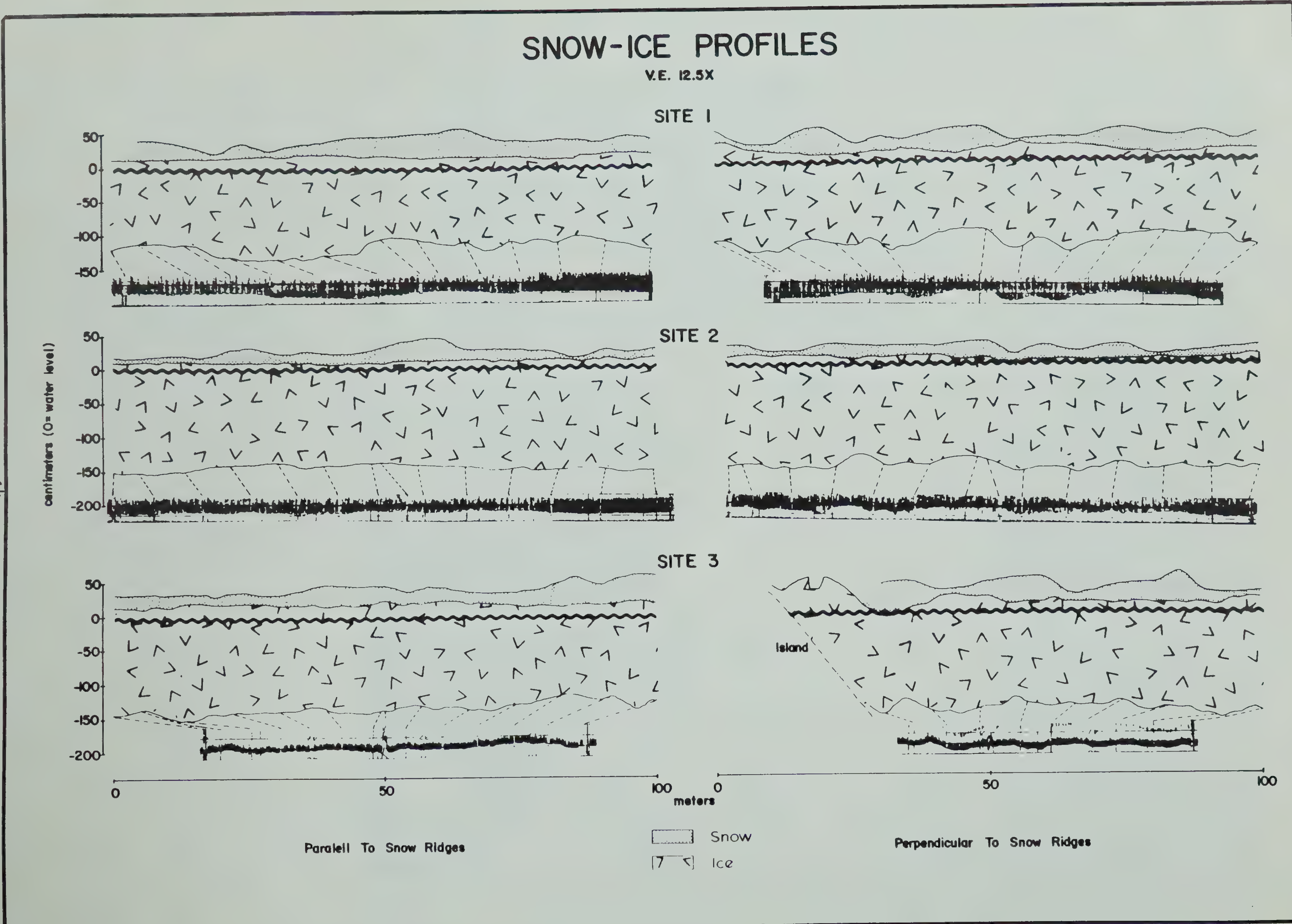

Figure 5. Profiles of snow and ice depth and thickness relative to sea level, at each of the three sites. The profiles on the left are oriented parallel to the snow ridge pattern and those on the right are perpendicular. Under each profile is the upward-looking fathometer trace of the relief on the under-ice surface.

TABLE I - DATA SUMMARY

	Snow Depth				Ice Thickness				Subice Surface - Draft				Snow/ice Interface - Freeboard			
Site #1	Average	Max.	Min.	Range	Average	Max.	Min.	Range	Average	Max.	Min.	Range	Average	Max.	Min.	Range
$\parallel$ to Sastrugi	25 cm	42	10	32	133	152	119	33	123	140	110	30	10	19	4	15
$\perp$ to Sastrugi	23	41	6	35	135	155	114	41	125	140	108	32	10	23	3	20
Average for site	24	42	6	36	134	155	114	41	124	140	108	32	10	23	3	20
Site #2																
$\parallel$ to Sastrugi	15 cm	33	4	29	157	165	146	19	149	157	141	16	8	11	3	8
$\perp$ to Sastrugi	15	24	6	18	157	167	145	22	151	161	135	26	7	12	1	11
Average for site	15	33	4	29	157	167	145	22	150	161	135	26	7	12	1	11
Site #3																
$\parallel$ to Sastrugi	23 cm	40	13	27	152	169	131	38	138	154	118	36	14	20	9	11
$\perp$ to Sastrugi	25	48	7	41	158	167	134	33	143	158	128	30	11	23	-7	30
Average for site	24	48	7	41	153	169	131	38	140	158	118	40	13	23	-7	30
Kovacs (197	Not measured				191	201	110	31								

gathered at 5 m intervals. The data used for these graphs were then used to determine a correlation coefficient between ice thickness and snow depth and the best fit line for the data at each site. At all three sites studied there was a negative correlation between ice thickness and snow depths measured along the trenches. The plots and the correlation coefficients show that a good correlation exists at Sites 1 and 3. The correlation at Site 2 is weaker as shown in Figure 6.

Morphologic Comparison of Snow and Under-ice Surface

The results show a good correlation between the morphologic patterns found on the snow surface and the morphologic patterns found on the undersurface of the fast ice. The quality of side-scan records and aerial photography were such that precise correlation feature for feature was not possible with our data.

The surface of the sea ice in the study areas was covered with snow in the form of ridges and troughs which were scoured and eroded forming sastrugi. The snow ridges and sastrugi showed an orientation of 70 degrees. Snow ridge wavelength, as observed in aerial photography, was typically 10 m; although values ranged from 5 m to 20 m. The character of the snow surface, as observed from aerial photography, is shown in Figure 7a and the interpreted ridge-crest pattern from this photography is shown in Figure 8a.

Side-scanning sonar records of sub-ice reflectors showed linear orientation of 70 degrees although the variability was greater than with the snow ridge orientations. Although the crests were less clearly defined on the sub-ice record than on the aerial photographs, wavelengths between crests were typically 10 m and ranged from 5 to 18 m - similar to the snow surface character. A sonograph from test

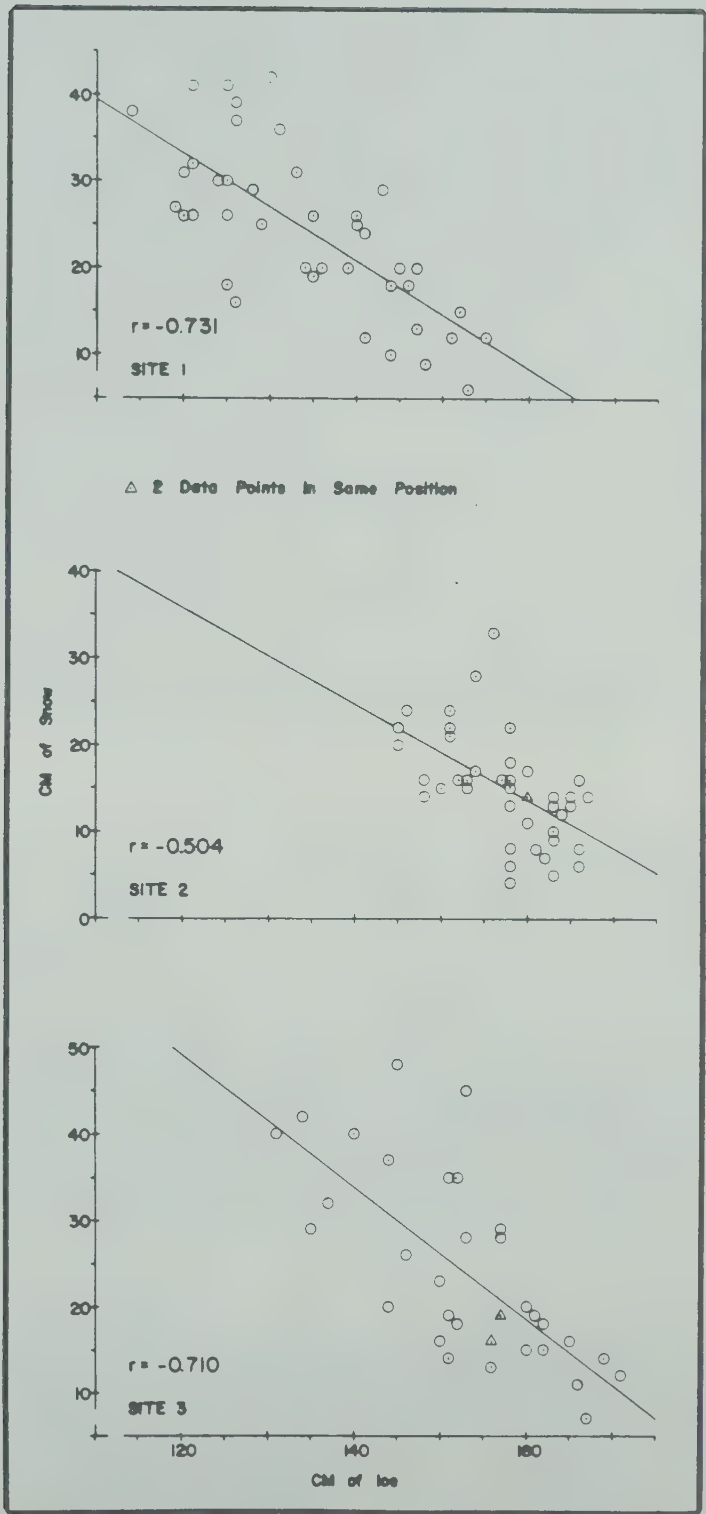

Figure 6. Scatter plots, best line fit and correlation coefficients for ice thickness and snow depth values at each of the three sites.

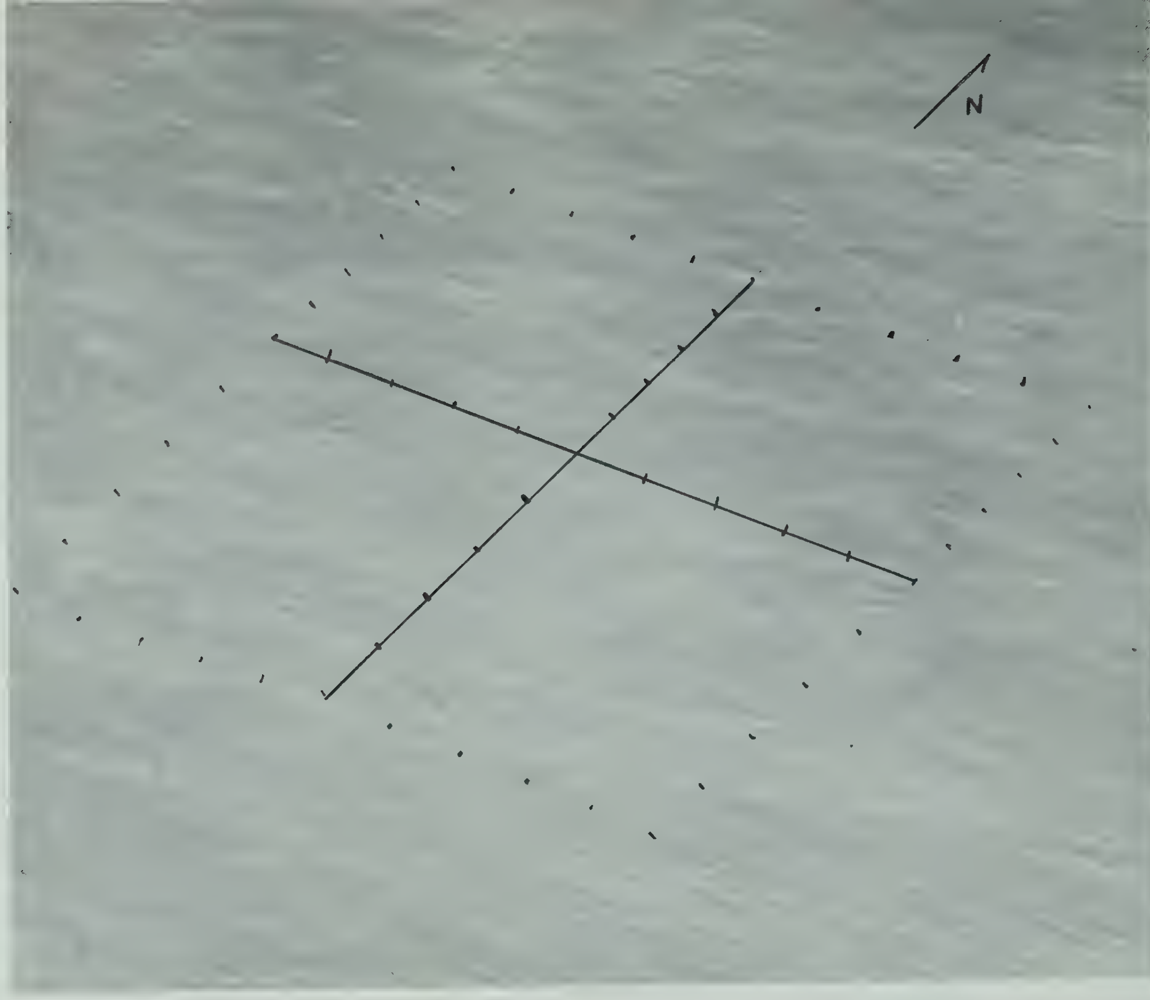

Figure 7a. Aerial photograph of Site 2 prior to plowing and trenching, showing the snow ridge pattern. The 100 m^2 grid and the cross have been added.

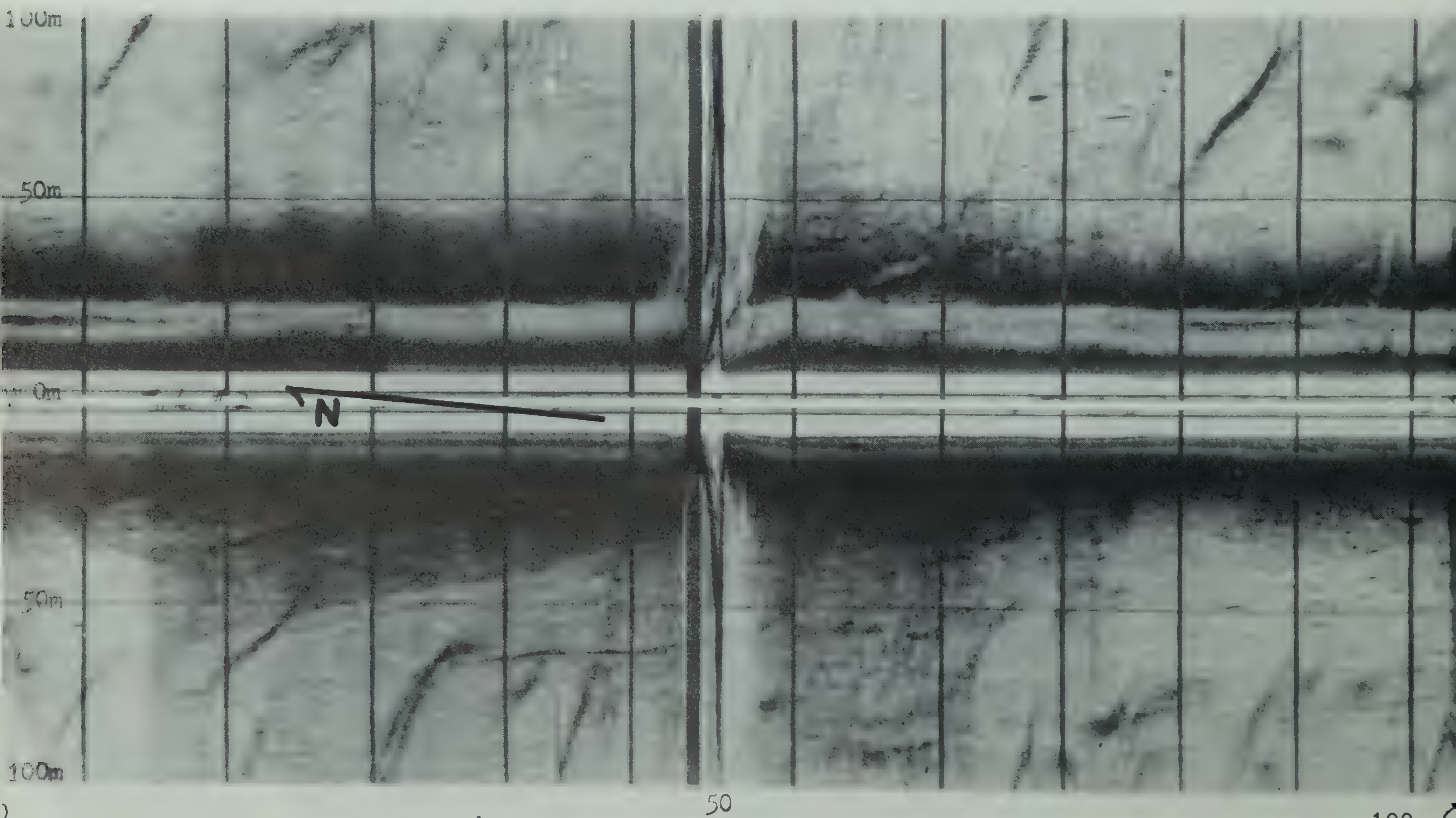

Figure 7b. Sonograph from the upward-looking sonar at Site 2 taken along the trench running perpendicular to the snow ridge pattern showing the reflections from the ridges on the undersurface of the ice.

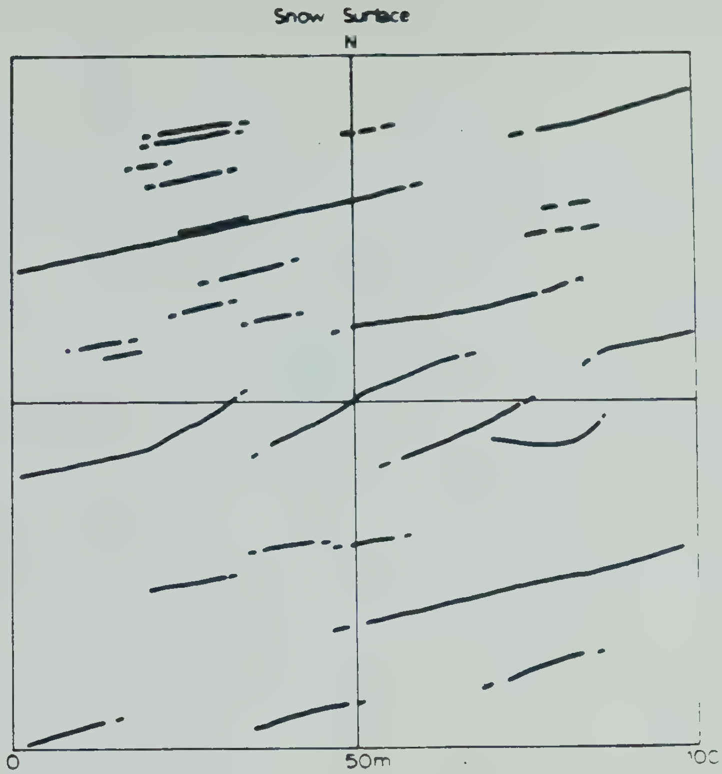

Figure 8a. Snow ridge pattern interpreted from the aerial photograph shown in Figure 7a.

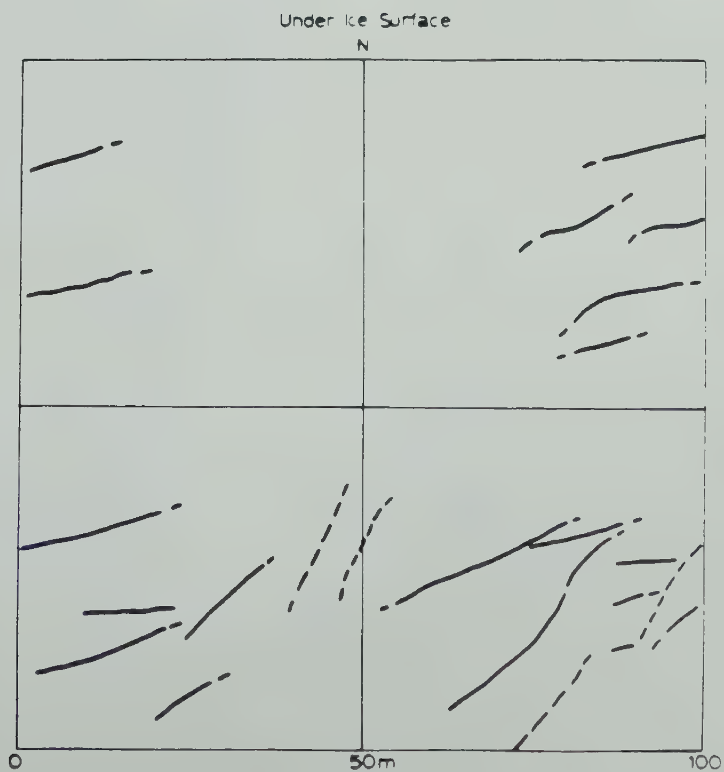

Figure 8b. Ridge pattern on the undersurface of the ice at Site 2 interpreted from the sonographs of Figure 7b.

Site 2 showing the reflectors on the undersurface of the ice is shown in Figure 7b and the interpreted crest orientation location is shown in Figure 8b.

Stability of Snow Ridges

Repetitive surveys and time lapse photography indicate that the basic ridge and trough snow pattern is stable. At Sites 1 and 3 the snow depths along the cross were remeasured after a northeasterly wind redistributed much snow on the sea ice. During the interval between these measurements wind velocities were above 10 m/sec (20 knts) and gusts in excess of 15 m/sec (30 knts) were recorded at the Deadhorse airport for a period of 12 or more hours. Although these winds moved considerable snow, the profiles before and after the wind events at both test sites were essentially unchanged. Ridges and troughs coincided before and after the wind events. Additionally, simple downwind extension of snow ridges was not observed. The changes in snow depth as measured at Sites 1 and 3 are illustrated in Figure 9 along with the wind data which show the wind events between the two surveys.

The time lapse camera record illustrated transient snow movement events yet also attested to the stability of the snow ridges. On May 2nd, when wind velocities at the Deadhorse airport were in excess of 10 m/sec (20 knts), the film showed snow spots of irregular outline and drifts with a barchan-like form migrating downwind temporarily covering and uncovering stationary snow ridges. Between the 6th of May and the 15th of May wind speeds in excess of 10 m/sec (20 knts) were recorded and a similar movement of snow spots was observed although the barchan-like forms were less well developed; rather, ripple-like features transverse to the wind were developed. The sastrugi-sculptured snow ridges remained essentially unchanged.

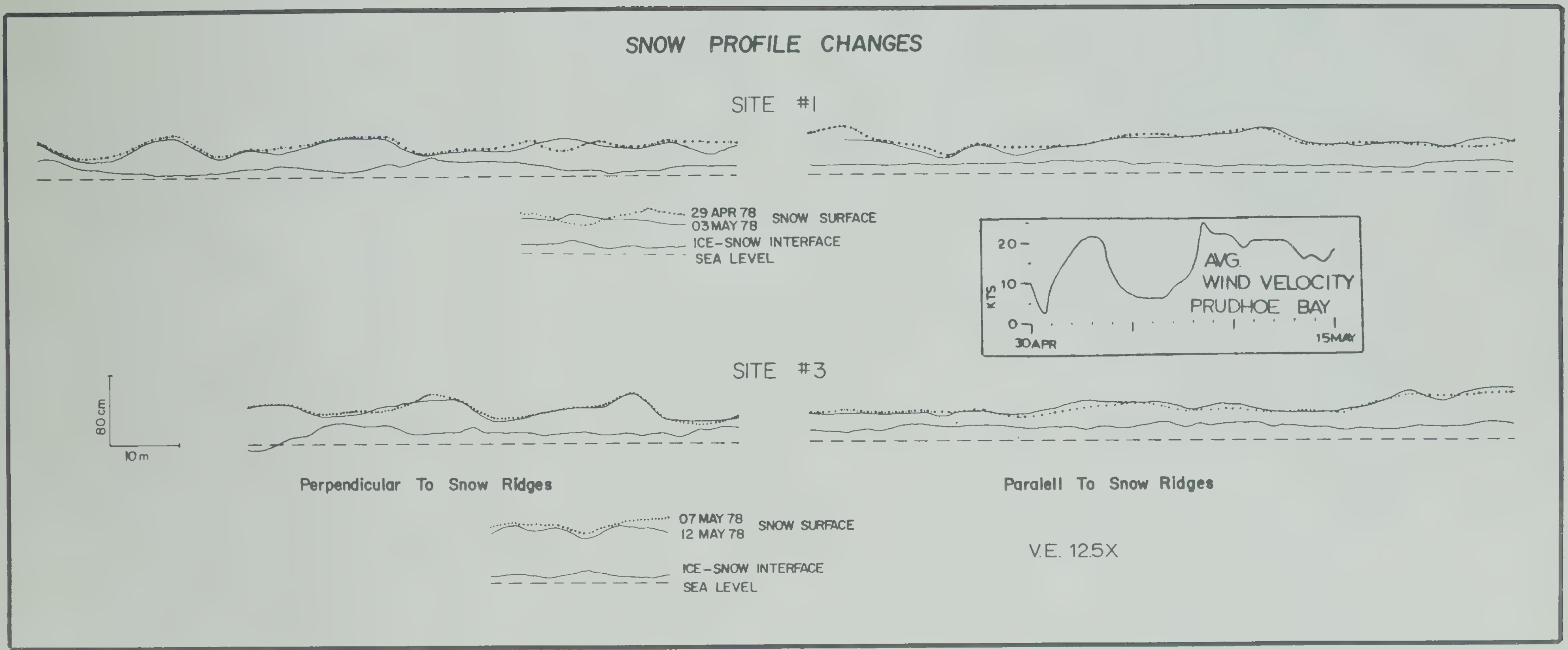

Figure 9. Replicate snow depth measurements at Sites 1 and 3 showing the small changes occurring during two wind events with velocities in excess of 20 knots. Wind data from the airport at Prudhoe Bay is shown in the inset.

Diving Observations

Diving observations on the undersurface of the ice were surprisingly similar at the three distinctly different environments. Observations were hampered by low light levels under the ice due to the large quantity of sediment included in the upper part of the ice canopy. The broad undulations seen by side-scan and upward-looking sonar are not visible to the eye, even with 5-10 m visibility. Smaller undulations, forming 5 to 8 cm deep diver-exhaust air pools, 2 to 6 m in diameter, were observable only because of the trapped air. The smallest air pools outlined 2 x 10 cm long depressions that are about 0.5 to 1 cm deep, and oriented parallel to the ice crystal fabric. Under proper lighting this fabric was distinct, and over distances of 1 to 3 m, parallel.

Randomly distributed ice stalactites, about 2 m apart, and 3 cm to 50 cm long were the most distinct sub-ice features. These stalactites consist of a very fragile crystal matrix. The large ones apparently have hollow cores. The stalactites mark brine channel openings from 0.5 cm to 8 cm in diameter (large enough to insert all four fingers of a gloved hand). One of the stalactites we observed closely was about 10 cm long and was actively spilling a plume of brine, 10 to 20 cm long, marked by light diffraction. The large stalactites resulted from the drainage of water we placed on the ice surface during trench-making activities. Under the prevailing conditions of open brine channels, our breath exhaust leaked through the fast ice very rapidly so that 3 m diameter, 5-8 cm deep air pools disappeared in several minutes while bubbling was observed on the ice surface as the air escaped.

In summary, our results show a strong correlation between measured

In summary, our results show a strong correlation between measured snow depth and ice thickness and a good correlation between the morphology as expressed by the orientation and the wavelength of snow ridges and under-ice surface relief. The observed stability of snow ridges indicates that the surface snow pattern is of prime importance in determining the morphology of the undersurface of the ice in several environments of the fast ice in the Prudhoe Bay area.

DISCUSSION

The correlation and character of snow and ice relief has implications regarding the stability of snow patterns, the potential for under-ice oil entrapment, and the physical differences between the different sites studied.

If snow ridges actively migrate during winter, their insulating effect on the sea ice would be mitigated as they migrated across the surface, tending to smooth out heat transfer differences. Consequently differences in ice thicknesses would be less and unrelated to snow patterns. The correlation between ice thickness and snow depth, and similarities between surface snow patterns and under-ice relief suggest that the snow ridge and trough character is stable throughout most of the winter. This is contrary to the intuitive observation that the wind-faceted sastrugi and drifting snow indicate these bedforms are in constant motion through the winter. Instead, it appears, as shown in our time-lapse photography, that snow spots and/or barchans are the mobile manifestation of a small segment of the snow cover at times of wind-driven snow events. Futhermore, it appears that the snow in transit does not affect the basic distribution of snow ridges and troughs.

The snow-ice correlation also suggests that the intermittent presence and movement of snow patches is apparently less important in the overall thermal regime than the underlying snow ridge. The effect of moving snow patches may be to increase the average insulation effect on the sea ice. The data also suggest that the oriented snow ridges and troughs probably form early in the ice growth season to allow sufficient time for development of ice thickness variations. This also suggests that northeasterly winds are prevalent early in the season and maintain themselves as the dominant force throughout the winter (Aagaard, 1978). A variety of winds from other directions might be expected to complicate the snow pattern and diffuse the correlation between ice thickness and snow depth.

An estimate was made of the potential for oil entrapment in the troughs on the undersurface of the fast ice. An assumption had to be made regarding the voids to be considered for this calculation. As oil reaches the undersurface of the ice it will spread laterally, equalizing at some "depth" beneath the ice depending on the elevation of "passes" between adjoining ridges and troughs on the under-ice surface. Intuitively it seemed reasonable to assume that "passes" in the under-ice ridge and trough pattern would exist near the mean draft computed for the ice. Thus the voids determined from our calculations are based on the relief above the computed mean draft at each site. Our calculations differ from those done by Kovacs (1977) in that we use the draft variations of our ice rather than ice thickness to compute voids. Draft values take into account the isostatic effects and result in lower volume calculations. The results of these calculations show a considerable difference between the three sites but all sites have values of the same order of magnitude (25 to 47 x 10^3 m^3/km^2) yet are

comparable to the values obtained by Kovacs in 1977 (Table II). This suggests that in the fast ice zones where ice is presumed to be flat, a considerable volume of oil could be contained on the undersurface of the fast ice in a rather small area (600 to 1200 barrels per acre).

Each site appears to be a unique physical environment as was initially suggested when the reasons for choosing these sites was discussed. Site 1 showed a good correlation between snow depth and ice thickness and is believed to represent the stability of the ice in Prudhoe Bay. However, the average ice thickness and computed ice thickness were thinner at Prudhoe Bay than at the other two sites by about 20 cm (Table II), reflecting the fact that high sub-ice salinities resulted in lower freezing temperatures and a slower rate of ice growth than at the other sites.

The average snow depth at Site 1 is the same as at Site 3 but deeper than at Site 2. On the tundra the average snow depth was noted by Benson and others (1974, p. 24) to be 32 cm. Our sites closest to the tundra, Sites 1 and 3, show 24 cm average snow depth while our site furthest from shore, Site 2, shows only 15 cm of snow depth, implying a gradient of increasing snow depths in an onshore direction. This gradient is believed to result from the variability of the terrain on which the snow is accumulating. A terrain with a great deal of relief would naturally accumulate a greater average snow depth due to the presence of larger traps, whereas a terrain of low relief would provide less obstruction to the flow of blown snow. Indeed this is what we observed, in that the observed range and freeboard is least at our offshore site, being about 10 cm, while at the inshore sites the range is about 20 cm. The relief on the tundra is even greater (Benson and others, 1975).

TABLE II

SITE COMPARISONS

	Snow Depth Ice Thickness Correlation Coefficient	Ice Thickness Computed for '0' Snow depth	Observed Average Ice Thickness	Observed Average Snow Depth	Observed Average Freeboard	Sub-ice Water Temp.	Sub-ice Water Salinity	Sub-ice Voids Above Average Draft
Site # 1 Prudhoe Bay	-0.73	173 cm	134 cm	24 cm	10 cm	<-2.0°C	>64°/oo	47,000 m^3/km^2 (12 00 bbls/acre
Site # 2 Stefansson Sound	-0.50	184 cm	157 cm	15 cm	7 cm	-2.0°C	38°/oo[a]	25,400 m^3/km^2 (650 bbls/acre)
Site # 3 Tidal Inlet	-0.71	184 cm	153 cm	24 cm	13 cm	-1.6°C	38°/oo	36,200 m^3/km^2 (920 bbls/acre)
Kovacs, 1977			190 cm					27,500 m^3/km^2

a) measured 15 km to E in Stefansson Sound

At Site 2 there is a weaker correlation between ice thickness and snow depth as compared with the other two sites. Furthermore, this site has the smallest value for sub-ice voids. We suggest that ice motion probably occurred here early in the ice growth season. Even a small rotation could cause snow patterns to be realigned and new areas of greater or lesser insulation to develop, thus mitigating some of the early season thickness variations. As a result, late season correlations of ice thickness and snow depth would not be as well devloped.

Site 3 is characterized by a good correlation between snow depth and ice thickness and by an extreme variation in freeboard. The snow depth-ice thickness correlation suggests strongly that currents are less effective in controlling ice thickness than is the insulation effect of snow. It is interesting to note this conclusion in light of the recent work by Kovacs and others (1978), which shows a strong relationship between ice crystal orientation and sub-ice current directions. Evidently there is no strong correlation between ice thickness, under-ice relief and crystal orientation. The 30 cm range in freeboard, from 23 cm above water level to 7 cm below, suggests that the ice in this tidal inlet may be under stress from motion early in the growth period or from stresses developed during the growth of the ice canopy due to confinement between the islands.

The geologic implications of the surface snow pattern and its stability and the resulting under-ice surface ridge and trough morphology are minor. Reimnitz and others (1978), have described windblown sediment accumulations that occur only in the upper parts of

the snow on the fast ice. In light of the stability of the snow ridge and trough topography, eolian material would be found only on the upper surface of the more stable snow ridges and associated with snow spots. Toimil and Reimnitz (1978), show a pattern of herringbone reflectors on side-scanning records which they ascribe to helical flow. The transverse wavelength of these features is about 10 m which corresponds to the 10 m wavelength between ridges on the undersurface of the ice. This ridge and trough system may be responsible for the spacing and the origination of the helical flow, whatever the source of current.

Implications for Offshore Development

Several implications become apparent for ice management in an offshore development situation. Ice thickness can be controlled by varying snow depth. Maintenance of a snow-free ring around the development site could cause ice to grow thicker and obstruct outward flow of oil. If the removed snow were piled deeper on an inner ring, the ice would be insulated, decreasing ice growth, and causing a natural ring-shaped pocket to form on the undersurface of the ice and floating sub-ice oil would gather inside of the thicker ice ridge.

If an ice spill occurred in a natural snow and ice environment, accumulations of oil would be great under snow ridges. As these ridges will have the thinnest ice and the greatest accumulation of oil, a logical approach to clean-up might be to drill holes in the snow ridges. Additionally, the data suggest that the predominant direction of oil migration would parallel the surface snow-ridge pattern. One would not expect a circular oil spread but rather a more elongate oil spread paralleling the surface snow pattern.

REFERENCES

Aagaard, K., 1978, Physical oceanography and meterorology, in Weller, G., Norton, D., and Johnson, T, eds., Interim Synthesis Report: Beaufort/Chukchi Sea Environment, National Oceanic and Atmospheric Adm., Boulder, CO, p. 56-100.

Barnes, P.W., Reimnitz, Erk, and Smith, Greg, 1977, Some coastal oceanographic observations--Beaufort Sea, Alaska, U.S. Geol. Survey Open-File Rept. 77-477, p. A1-9.

Benson, C.S., Holmgren, B., Trabant, D., and Weller, G.,1974, Physical characteristics of seasonal snow cover in northern Alaska, Proc. of the Western Snow Conference, 1974, University of Alaska, Fairbanks, Alaska, p. 58-63.

Benson, C.S., Timmer, R., Parrish, S., and Holmgren, B., 1975, Observations on the seasonal snow cover of Prudhoe Bay, Alaska during 1972, in Brown, J., ed., Ecological Investigations of the Tundra Biome in the Prudhoe Bay Region, Alaska, Biological Papers of the University of Alaska, Special Rept. 2, p. 13-5.

Brown, R.F., Dickens, D.F., and Overall, J.G., 1975, The interaction of crude oil with arctic sea ice, Beaufort Sea Technical Report no. 27, Beaufort Sea Project, Dept. of the Environment, Victoria, B.C., Canada, 149 p.

Kovacs, A., 1977, Sea ice thickness profiling and under-ice oil entrapment, Offshore Technology Conference Proc., v. 3, p. 547-554.

Kovacs, A., and Mellor, M., 1974, Sea ice morphology and ice as a geologic agent in the southern Beaufort Sea, in Reed, J., and Sater., J., eds., The Coast and Shelf of the Beaufort Sea, Arctic Inst. of North America, Arlington, Va., p. 113-161.

Kruchinin, Y.A., 1962, Microrelief of the snow surface on the Lazerev ice shelf, Soviet Antarctic Expedition Information Bull., v. 4 (2), p. 77-79.

Schell, D.M., 1974, Seasonal variation in the nutrient chemistry and conservative constituents in coastal Alaskan Beaufort Sea waters, University of Alaska Institute of Marine Science, Rept. R74-1, p. 217-281.

Toimil, L.J., and Reimnitz, Erk, 1977, A Herringbone pattern of possible Taylor-Görtler-type flow origin seen in sonographs, U.S. Geol. Survey Open-File Rept. no. 77-477, p. D-1.

Zubov, N.N., 1943, Arctic Ice, Translated by Naval Oceanographic Office and American Meteorological Society, 1963, pub. Naval Electronics Laboratory, San Diego, Ca., 491 p.

GPO 689-035